

Crashworthiness Assessment of Square and Circular Crash Boxes with Single and Dual Screw-Groove Triggers under Axial Impact¹ <https://orcid.org/0000-0001-5376-7502>; ² <https://orcid.org/0009-0001-4409-0066>;^[1]Teddy Samuel R, ^[2]Jaikumar Mayakrishnan^[1] PhD Research Scholar, Hindustan Institute of Technology and Science, ^[2] Professor, Hindustan Institute of Technology and Science, Chennai, India^[1] teddysamuel.312@gmail.com ^[2] mjaikumar@hindustanuniv.ac.in*Corresponding Author: mjaikumar@hindustanuniv.ac.in

Abstract— This study investigates the design and development of square and circular crash box models with enhanced crashworthiness through the investigation of screw-groove combinations. Two designs were investigated: one with a single screw positioned in two grooves, and the other with two screws positioned in four grooves. Crash boxes made out of aluminum alloy 5052 were manufactured and strengthened using thick mild steel sleeves. These were tested numerically, LS-DYNA, and experimentally, by impact test at 4.2 m/s with a 700 kg mass. The most valuable parameters that were examined were energy absorption (EA), specific energy absorption (SEA), peak force, mean crushing force and crush force efficiency (CFE). Experimental results showed that transitioning from two to four grooves increased EA by 3–5× and improved CFE from ~54% to ~70%, indicating more stable progressive crushing. Square crash boxes consistently outperformed circular ones w.r.t. EA (up to 24% higher for the four-groove design), while circular designs exhibited better load uniformity. Simulations captured overall deformation modes but underestimated peak forces and CFE compared to experiments, primarily due to idealized material modeling and boundary conditions. The results verify that geometry and screw-groove placement play a critical role toward control of crash energies with a four-groove square crash box having the best energetic crash-handling capacity in high-impact zones. The numerical experimental method employed in this study can serve as a springboard for optimizing - crash box design to further enhance the safety of a vehicle occupant.

Keywords— Axial Impact Testing, Crashworthiness, Energy Absorption, LS Dyna Simulation, Screw-Groove Design**INTRODUCTION**

Crashworthiness is the ability of a vehicle structure to protect its occupants upon impact by absorbing and dissipating energy caused by such an impact, and it is a basic principle of automotive engineering. Crash boxes are energy-absorbing structures that mitigate the severity of impacts in vehicles by deforming in a controlled manner to absorb kinetic energy [1]. Typically integrated into the front or rear structure of the vehicle, they help minimize the transmission of impact loads to the occupant compartment [2]. Crash boxes have undergone extensive development over the years, with research and studies aimed at optimizing their geometry, choosing suitable materials, and optimizing structural designs for better energy absorption, crush force efficiency, and load distribution [3, 4]. Traditional crash box designs typically utilize simple tubular geometries, such as circular or rectangular tubes, due to ease of manufacture and efficiency in energy dissipation under axial loads [5]. However, the performance of such structures is undermined by limitations such as buckling instability and uneven load distribution, endangering occupant safety [6]. To overcome these limitations, new design approaches have been explored, including the introduction of grooves, cut-outs, or triggers, with the prime objective of inducing controlled deformation and improving crashworthiness [7, 8]. Of these approaches,

screw-groove designs have been identified as a viable alternative as they induce progressive crushing and enhance energy dissipation by controlling deformation through predefined paths [9, 10]. The application of screw-groove configurations in crash boxes offers a new solution for energy absorption. The application of screws in grooves offers localized deformation, thus improving the stability of the crushing mechanism and reducing peak forces [11]. Previous studies have focused on single screw-groove systems, demonstrating their superior effectiveness in energy absorption compared to conventional tubular configurations. [12, 13]. However, the potential of dual screw-groove configurations, with multiple screws and grooves, has not been comprehensively studied. Expanded research in this area has the potential to offer improved load distribution and higher energy absorption capacity, especially under diverse impact conditions [14, 15].

Material selection is a primary factor that influences crash box performance. Aluminum alloys, especially Al5052, are widely employed due to their favorable strength-to-weight ratios and high energy absorption properties [16]. Mild steel is commonly used due to its cost-effectiveness and ductility, making it well-suited for crash box applications [17]. Material selection, together with structural design, critically influences crashworthiness metrics such as specific energy absorption (SEA), peak crushing load, and crush force efficiency [18]. Finite Element Method (FEM) simulation, generally performed using software packages such as LS-DYNA, are now irreplaceable tools for crash box performance evaluation under dynamic loading conditions [19]. FEM simulations enable researchers to investigate the influence of design parameters, such as groove geometry and impact speed on crashworthiness, thus minimizing the use of large-scale physical testing [20]. The current study aims to evaluate the crashworthiness properties of circular crash boxes with single and double screw-groove configurations using Al5052 Aluminum alloy and mild steel as the major materials. By analyzing the functionality of these configurations under axial impact at different speeds using Finite Element Method (FEM) simulations in the LS-DYNA environment, this study investigates the performance of these configurations in terms of energy absorption and load distribution as they crash. As indicated in the abstract, the study hypothesizes that the double screw-groove configuration (two screws in four grooves)

will provide superior energy absorption and load distribution compared to the single screw-groove configuration. These findings are anticipated to inform the development of more efficient crash boxes, thereby improving occupant safety in vehicle collisions. The findings from this study extend current research in the field [1-20], offering a new insight into the optimization of the screw-groove configurations for the improvement of crashworthiness.

I. Materials & Methods

Materials

Aluminum Alloy 5052 was the material used in manufacturing crash boxes because of its high strength to weight ratio, corrosion resistance and ease of formation. The alloying compound mainly consists of aluminum and magnesium (2.2- 2.8%) and chromium (0.15- 0.35 %). The mounting sleeves, screws and nuts were made of mild steel (MS_MAT_20) having a yield strength of 350 MPa and Young's modulus of 200 GPa in order to create greater stiffness and stability for load transfer.

2.2. Crash Box Geometry: Square vs. Circular Designs Two geometries of crash box were discussed; a square cross-section and a box of circular cross-section that were built to display similar rigidity cross-sectional stiffness. To determine the wall thickness, relevant literature was consulted, which reported a value of 2.5 mm [21-27].

Crash Box Geometry

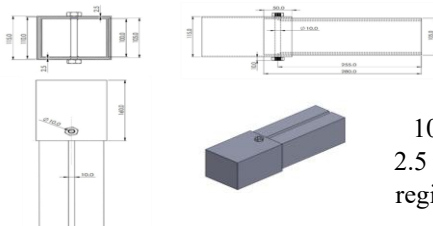


Fig. 1, Detailed Dimensional Drawing of the Square Crash Box incorporating two longitudinal grooves. Overall length: 280 mm; external cross-section: 100 × 100 mm; internal cavity: 95 × 95 mm; groove length: 255 mm; wall thickness: 2.5 mm. The solid front section measures 20 mm and the mounting sleeve attachment region at the rear have a length of 160 mm

Specimen 2 - Square Crash Box (4 Grooves)

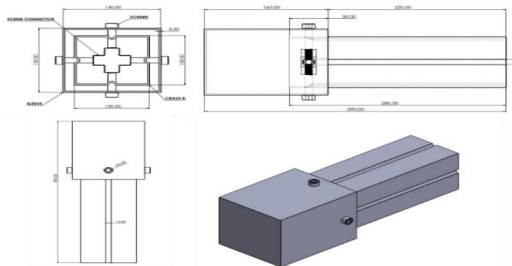


Fig. 2, Detailed Dimensional Drawing of the Square Crash Box incorporating four longitudinal grooves. Overall length: 280 mm; external cross-section: 100 × 100 mm; internal cavity: 95 × 95 mm; groove length: 255 mm positioned on all four faces; wall thickness: 2.5 mm. The solid front section measures 20 mm, and the mounting sleeve attachment region at the rear has a length of 160 mm.

Specimen 3 – Circular Crash Box (2 Grooves)

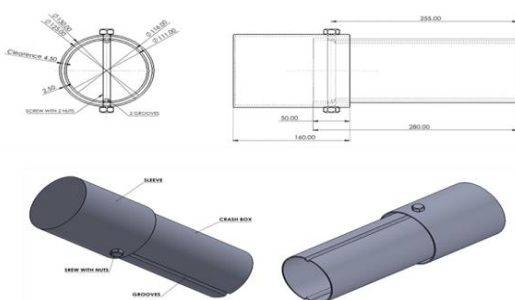


Fig. 3, Detailed Dimensional Drawing of the Circular Crash Box incorporating two longitudinal grooves. Overall length: 280 mm; outer diameter: 116 mm; inner diameter: 111 mm (wall thickness 2.5 mm); groove length: 255 mm positioned along opposite sides. The crash box is housed in a 160 mm, long mounting sleeve of 130 mm outer diameter. Mounting features match the square crash box design, with 10 mm wide screw slots, a solid front section of 20 mm, and a solid rear section of 130 mm to ensure comparable assembly and load transfer characteristics.

Specimen 4 - Circular Crash Box (4 Grooves)

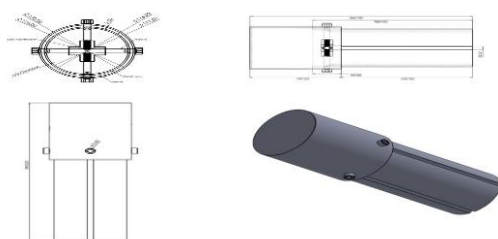


Fig. 4, Detailed Dimensional Drawing of the Circular Crash Box incorporating four longitudinal grooves. Overall length: 280 mm; outer diameter: 116 mm; inner diameter: 111 mm (wall thickness 2.5 mm); groove length: 255 mm positioned equally on all four quadrants. The crash box is housed in a 160 mm long mounting sleeve with an outer diameter of 130 mm. Mounting features are the same as for the square

and two groove circular designs, including 10 mm wide screw slots, a 20 mm long solid front section, and a 130 mm long solid rear section to ensure comparable assembly and load transfer conditions.

Specimen 5 - Screws and Nuts for Square crash box

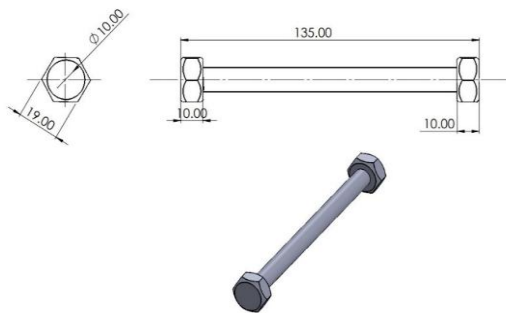


Fig. 5, Detailed Dimensional Drawing of the Screw and Nut Assembly used for the square crash box mounting. The screw has a nominal diameter of 10 mm with a 1.5 mm pitch conforming to the ISO M10 thread specification. The length allocated for the square crash box mounting is 135 mm, while for the circular crash box assembly it is 150 mm. The nut dimensions correspond to the M10 standard to ensure secure fastening and consistent load transfer during impact testing.

Specimen 6 - Screws and Nuts for Circular Crash Box

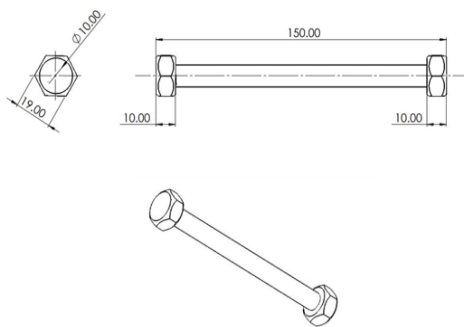


Fig. 6, Detailed Dimensional Drawing of the Screw and Nut Assembly used for the circular crash box mounting. The screw has a nominal diameter of 10 mm with a 1.5 mm pitch in accordance with the ISO M10 standard thread specification. The total length allocated for the circular crash box fastening is 150 mm. The nut dimensions conform to the ISO M10 standard to ensure reliable joint integrity and consistent load transfer during assembly and impact testing.

Pre-calculations and Structural Analysis

Pre-calculations were conducted to assess the structural behavior of the crash box under fixed end loading, providing an analytical baseline prior to finite element simulations and experimental testing.

For a cantilevered crash box, the elastic tip deflection δ under an applied load P is given by the Euler–Bernoulli beam equation:

$$\delta = (W_{\text{Half}} \times L^3) / (3E \times I) \text{ ----- (1)}$$

Where,

W_{Half} = Half the weight of the front structure (in Newtons)

L = Length of the crash box (in meters)

E = Young's modulus of the material (in Pascals)

I = Moment of inertia of the crash-section (in m⁴)

The cross-sectional properties were used to calculate load, reaction forces, and the position of the center of mass.

The center of mass X along the length of the crash box was calculated using the formula:

$$\text{Centre of Mass (X)} = (\sum(M_i * X_i)) / (\sum M_i) \text{-----(2)}$$

M_i = Force of each point

X_i = Position of each force from a reference point (Reference point is A)

Table 1 - Data for Centre of Mass Calculation of Crash Box

Point	Force M _i (N)	Distance from AA, X _i (m)	Moment M _i ×X _i (N·m)
A	0	0	0
B	10	0.14	1.4
C	150	0.28	42

Fabrication of Crash Boxes

The crash boxes were fabricated from Aluminium Alloy 5052 with a uniform sheet thickness of 2.5 mm, ensuring high dimensional accuracy and minimal material wastage.

Sheet Cutting

Precise dimensions were achieved by cutting the aluminium sheets in a sheet shearing machine resulting in a minimal amount of distortion and edge burrs.

Forming

The sheets were formed into the desired square and circular cross sections with a three bending roll machine, thus maintaining geometric homogeneity.

Welding

The misaligned sheets were welded together using Tungsten Inert Gas (TIG) welding, which is preferred due to its low incidence of weld defects, minimal heat-induced distortion, and reduced need for post weld finishing.

Groove Creation

Longitudinal grooves in the walls of the crash box were made with multi stage punching to obtain a high degree of accuracy. These grooves act as deformation initiators, enabling a controlled progressive collapse under impact.

Assembly Preparation

Bolt holes for the mounting bolts were accurately drilled to fit the fastening system and align with the mounting sleeves.

Surface Finishing

The ends of the assemblies were finished to enhance durability and corrosion resistance, thereby improving their service life both during crash testing and in real-world conditions. Precision, structural integrity and energy absorption were the primary objectives at every fabrication step, resulting in highly robust Aluminum Alloy 5052 crash boxes with excellent crashworthiness performance.

Fabrication Process Figures



Fig. 7, Rolling of Aluminum Alloy 5052 sheet using a three-roll bending machine



Fig. 8, Tungsten Inert Gas (TIG) welding of the rolled sheet to form the crash box body.

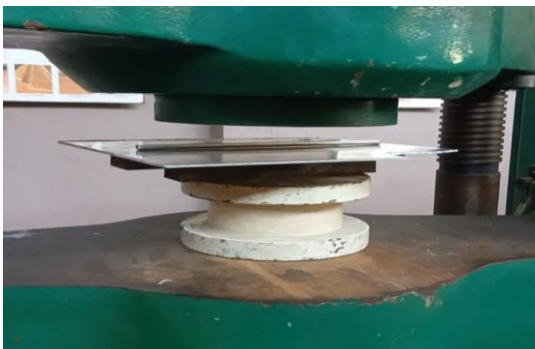


Fig. 9, Multi stage punching process for creating longitudinal grooves in the crash box walls.

Final Assembly of Crash Boxes

The individual components which were manufactured to look like crash boxes were put together with their own mounting sleeves, nuts and the bolts as per the ISO M10 fastening standard. This process provided a good fitment, alignment and prepared the structure to be crashworthy tested.



Fig. 10, Two Grooves Square and Circular Crash Boxes



Fig. 11, Four grooves Square Crash Box with Mounting Sleeve and Nut



Fig.12, Four grooves Circular Crash Box with Mounting Sleeve and Nut

Mechanical Testing: Tensile Test (According to ASTM E8/E8M-24)

To evaluate the mechanical performance of Aluminum Alloy 5052 used in the fabricated crash boxes, tensile testing was conducted at the groove section, a critical location for assessing local structural strength under applied loading conditions

Sample Preparation

A flat plate of Aluminum alloy of 5052 was fabricated and to simulate the actual scenario of the crash box groove, a longitudinal groove was punched on the specimen using a set of dissimilar to the one used in making the crash box. Subsequently, a thick section near the groove was extracted and machined into a standard tensile test specimen according to the geometric requirements of ASTM E8/E8M-24.

Testing Procedure

Tensile testing was performed using a Universal Testing Machine (UTM). Load was applied an incremental manner until the specimen failed. Load and displacement were recorded throughout the test to generate the stress–strain response, capturing both the elastic and plastic deformation characteristics.

Test Results

Table 2 provides a summary of the tensile test results for a grooved Aluminum Alloy 5052 sample, with literature values shown as the standard properties of the 5052H32 temper:

Table. 2 Tensile Test Results

Mechanical Property	Tensile Test Results	Standard 5052-H32 Results
Tensile Strength (MPa)	187 MPa	228 MPa
Yield Strength (MPa)	117 MPa	193 MPa
Elongation (%)	10%	12%

The reductions in tensile and yield strength observed in the grooved sample, relative to the standard values, are expected, as stress concentration and localized deformation induced by the groove contribute to these decreases. However, the ductility in the grooved region remains acceptable, as the elongation is close to the standard value Visuals



Fig.13, Aluminum Alloy 5052 Specimen with Groove prepared for Tensile Testing.



Fig.14, Universal Testing Machine setup used for the Tensile Test.



Fig.15, Machined AL 5052 Tensile Test Sample showing Gauge Length Near the Groove.



Fig.16, Stress Vs Strain

Computational Techniques

The crash behavior of the square and circular crash box was established by the method of finite element analysis (FEA) to predict their impact performance, deformation modes, and energy absorption capacity. The crash boxes were designed in Solid Works with a fixed wall thickness of 2.5 mm. The CAD geometries were then imported into Altair Hyper Mesh for structured meshing, which optimizes mesh quality by balancing accuracy and computational efficiency. The finite element simulations were performed using the explicit dynamic solver LS-DYNA. The material properties of Aluminum Alloy 5052 for the crash boxes and mild steel for the mounting components were assigned following relevant material models capturing elastic-plastic deformation behavioral rigid wall with an impact velocity of 4.2 m/s (15 km/h) was used to simulate the collision scenario. The impact or mass was set to 700 kg representing a standard vehicle mass. Boundary conditions fixed the crash boxes at the mounting sleeve end, replicating the experimental fixture constraints. This setup enabled detailed predictions of impact-induced deformation patterns, stress distributions, and the energy absorption behavior of the crash boxes under load. The selection of the 4.2 m/s impact velocity with a 700 kg mass for testing is based on benchmarking with established standards and practices in automotive crashworthiness research. An impact velocity in the range of 1–5 m/s is commonly used in low-velocity impact (LVI) studies, as it represents typical collision scenarios encountered in real-world automotive accidents, such

as those occurring in urban traffic or during vehicle-to-barrier tests. The 4.2 m/s velocity specifically falls within this widely accepted range and ensures a relevant assessment of structural integrity and energy absorption behavior for automotive components. The choice of a 700 kg mass for the impact or aligns with the standard reference mass for a passenger car used in various regulatory tests and comparative experimental setups. While modern electric vehicles (EVs) and sport utility vehicles (SUVs) may possess higher actual mass due to battery packs and larger body structures, the 700 kg value is conventionally employed for baseline comparisons to maintain consistency and enable evaluation with existing literature and safety protocols.

Material and Contact Modelling in LS-DYNA

The aluminum crash box was modelled using MAT_024 (Piecewise Linear Plasticity), incorporating isotropic hardening and strain-rate sensitivity via the Cowper–Symonds parameters as detailed above. The mild steel sleeve and screw components were modelled using MAT_020 (Plastic Kinematic) to account for bilinear elastoplastic behavior and higher yield stiffness. Material parameters were derived from the tensile tests performed on grooved AA5052 samples (Table 2) and validated against literature-reported dynamic properties for equivalent alloys.

In LS-DYNA, accurate prediction of crash deformation requires material definitions that go beyond basic elastic–plastic properties. In this study, Aluminium Alloy 5052 was selected as the primary crash-box material due to its favourable strength-to-weight ratio, excellent corrosion resistance, and high formability. Its chemical composition primarily aluminium with magnesium (2.2–2.8%) and chromium (0.15–0.35%), supports superior work-hardening behaviour, which is advantageous for progressive folding during impact. Mechanical properties obtained from tensile testing and literature include a Young’s modulus of 70 GPa, yield stress of 193 MPa, tensile strength of 228 MPa, elongation of 12%, and density of 2680 kg/m³. The mounting sleeves, screws, and fastening nuts were modelled using mild steel and implemented through MAT_020 Rigid to ensure efficient load transfer without deformation. This steel exhibited a yield strength of 350 MPa, tensile strength of 420 MPa, Young’s modulus of 200 GPa, and elongation of 15%.

To realistically represent deformation and failure, the aluminium crash-box material was defined using MAT_024 Piecewise Linear Plasticity, which enables modelling of non-linear plastic behaviour through multi-segment stress–strain curves. This material model supports strain hardening, strain-rate sensitivity, and up to 20 user-defined stress–plastic strain points, enabling accurate replication of the alloy’s post-yield response observed during tensile tests, including the reduced strength in grooved regions produced during fabrication. LS-DYNA’s MAT_024 parameters such as plastic hardening modulus, flow stress definition, and optional temperature dependency were incorporated to reflect the material’s behaviour under dynamic loading conditions typical of crash events. For components assumed undeformable, such as sleeves and bolts, MAT_020 Rigid was employed, simplifying computations while preserving realistic boundary interactions and constraints. The combination of experimentally calibrated aluminium plasticity, rigid steel interfaces, and advanced LS-DYNA material formulations ensures that the crash simulation captures essential deformation stages, elastic buckling, plastic folding, and densification, critical for evaluating crashworthiness performance.

The CONTACT_AUTOMATIC_SINGLE_SURFACE algorithm in LS-DYNA is widely employed for simulations involving large deformations and self-interaction of shell structures, such as thin-walled crash components. This contact formulation automatically detects and enforces contact between all potential slave and master surfaces within a defined set, making it particularly suitable for folding, buckling, and progressive crushing scenarios. Its performance is governed primarily by how LS-DYNA computes the interface stiffness, which controls the resistance applied when surfaces begin to penetrate. Two major approaches are available: the conventional penalty-based method, where stiffness is derived from material elastic properties and segment geometry, and the soft-constraint method, which replaces stiffness-based control with nodal mass and time-step-dependent constraints. The latter is often advantageous when dissimilar materials or distorted meshes are present, as it reduces excessive penetration and enhances numerical stability. Additional factors such as penalty scaling, contact thickness definition, viscous damping, and allowable penetration thresholds further influence the robustness and accuracy of the contact response, especially in regions with complex folding or sharp geometric features.

In practice, selecting appropriate values for these parameters is essential to ensure realistic structural behavior. The recommended workflow begins with the standard penalty formulation for cases involving similar materials, followed by using SOFT = 1 or SOFT = 2 when instability, high penetration, or contact noise is observed. Penalty scale factors and contact thickness must be tuned carefully, as overly small thickness values can compromise contact detection, whereas excessively high stiffness may induce artificial oscillations or reduce the stable time step. For crashworthiness studies, additional damping and controlled penetration limits help maintain stable contact forces throughout the crushing event. Overall, a well-calibrated CONTACT_AUTOMATIC_SINGLE_SURFACE setup enables accurate modelling of energy absorption and deformation progression, making it a reliable choice for analyzing thin-walled members subjected to impact loading.

Deformation Mode of Crash Boxes

The crash boxes that are deformed at different geometries and groove patterns differ as per the visualization in the following figures:

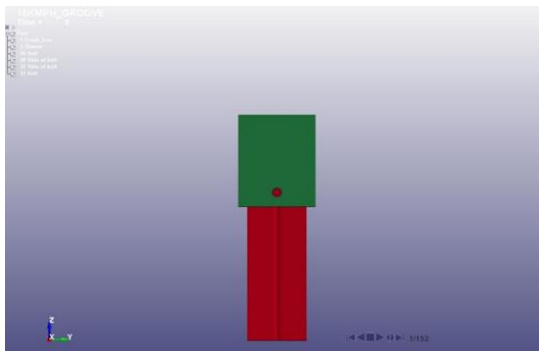


Fig.17, Initial Configuration of Square Crash Box with Two Grooves Before Impact

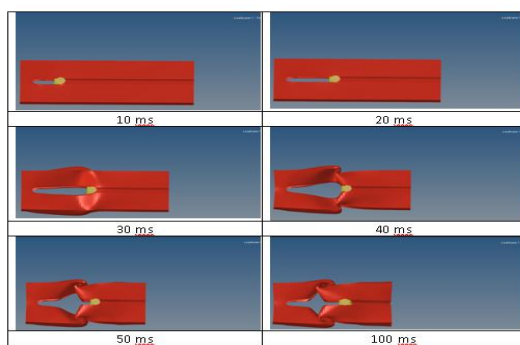


Fig. 18, Sequential Deformation Visuals of Two Groove Square Crash Box Derived from LS Dyna Simulations

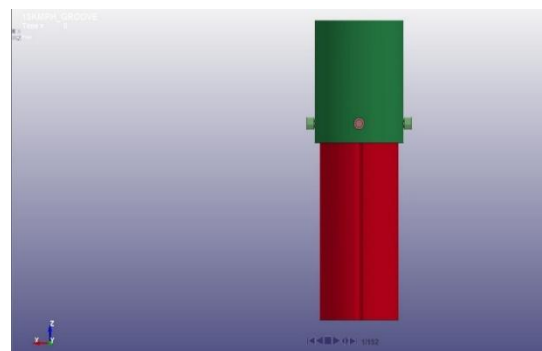


Fig.19, Initial Configuration of Circular Crash Box with Two Grooves before impact

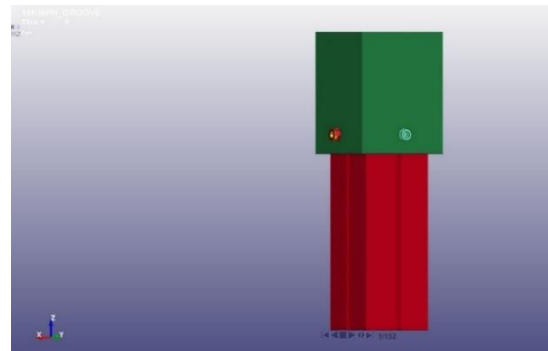


Fig. 20, Initial Configuration of Square Crash Box with Four Grooves Before Impact

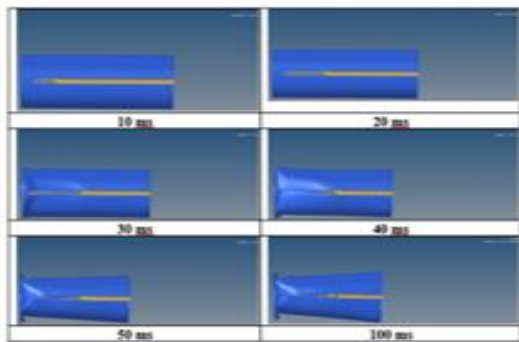


Fig. 21, Sequential Deformation Visuals of Two Groove Circular Crash Box Derived from LS Dyna Simulations

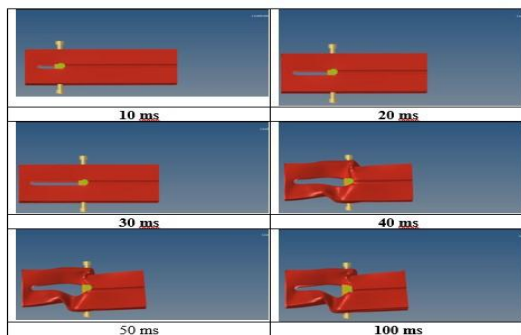


Fig. 21, Sequential Deformation Visuals of Four Groove Square Crash Box Derived from LS Dyna Simulations

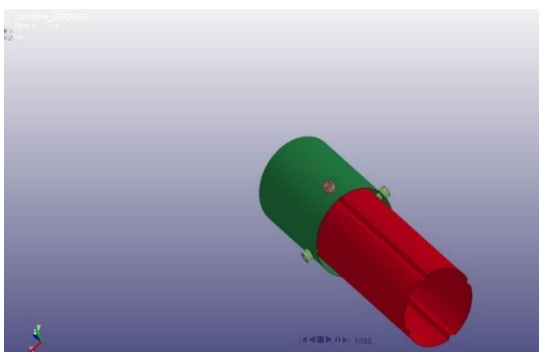


Fig. 23, Initial Configuration of Circular Crash Box with Four Grooves Before Impact

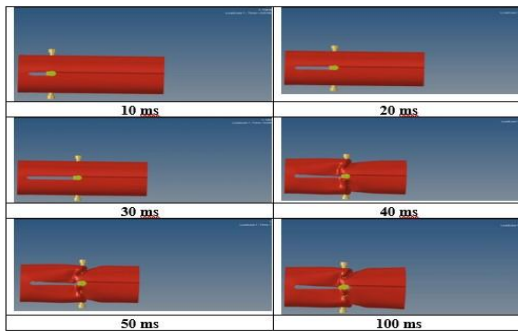


Fig. 24 Sequential Deformation Visuals of Four Groove Circular Crash Box Derived from LS Dyna Simulations

Compression Test and Results

A quasi-static axial compression test was used to determine the crashworthiness and energy absorption capability of the square and the circular crash boxes. The test simulates the crushing behavior of the crash boxes under impact conditions representative of automotive crashes, reinforced with comparable axial loading

The Procedure and Method of Setup Test

The crash boxes, all fabricated with a uniform wall thickness of 2.5 mm, were subjected to axial compression under controlled quasi static displacement or load conditions using a testing machine. The specimens were compressed longitudinally at a low strain rate to evaluate their progressive deformation behavior and energy absorption capability. During the tests, several key parameters were recorded: the load displacement response, which provides insight into deformation patterns and structural stiffness; the crushing strength, representing the maximum load a specimen can withstand without significant structural failure; the mean crushing load, which reflects the average load during progressive collapse and is indicative of stable energy absorption; the total energy absorption (EA), calculated as the area enclosed by the load displacement curve, quantifying the energy dissipated during crushing; and the specific energy absorption (SEA), defined as the EA divided by the mass of the crash box, offering a measure of absorption efficiency relative to weight.



Fig.25, square and circular crash boxes under compression test setup.

II. Results and Discussion

Summary of Simulation and Experimental Results

Shape	Config	D Sim (mm)	D Exp (mm)	EA Sim (kJ)	EA Exp (kJ)	SEA Sim (J/g)	SEA Exp (J/g)	MCF Sim (kN)	MCF Exp (kN)	Peak Force Sim (kN)	Peak Force Exp (kN)	CFE Sim (%)	CFE Exp (%)	LTI (Sim)	LTI (Exp)
Square	2 Grooves	54.9	46.2	156.18	1.09	222.2	1.55	2.84	23.59	28	47.16	59.06	50.04	0.6	0.5
Square	4 Grooves	52.7	75.4	165.55	3.62	235.5	5.15	3.14	48.01	57.7	60.06	60.06	79.90	0.6	0.8
Circular	2 Grooves	51.3	30.6	36.52	0.73	51	1.04	0.71	23.86	15.8	54.49	54.49	43.79	0.5	0.4
Circular	4 Grooves	54.4	51	249.14	2.91	354.1	4.15	4.58	57.06	69.3	70.19	70.19	58.15	0.7	0.6

Figure 26, presents a comparison between simulation and experimental values of Deformation (D), Energy Absorption (EA), Specific Energy Absorption (SEA), Mean Crushing Force (MCF), Peak Force (PF), and Crush Force Efficiency (CFE) for the four crash box configurations.

Observations

General Trends

For all crash box configurations, the experimental measurements of energy absorption (EA), specific energy absorption (SEA), mean crushing force (MCF), and crush force efficiency (CFE) were consistently higher than those obtained from the finite element simulations. The deformation values predicted by the FE model were generally within about 5 percent of the experimental measurements, indicating reasonable agreement in displacement prediction. However, the simulations substantially underestimated both the MCF and the peak force. For example, in the square two groove configuration, the simulated MCF was 2.84 kN compared to 23.59 kN in the experimental test, representing an underestimation of nearly 88 percent. Similar trends of under prediction were observed across all other configurations.

Energy Absorption (EA) and Specific Energy Absorption (SEA)

Experimental results demonstrated superior EA and SEA values compared to the simulations, with the most pronounced differences appearing in the four groove designs:

- Square four grooves: EA measured experimentally was 3.62 kJ versus 165.55 J in simulation (noting that differences in units or modeling assumptions may contribute to the magnitude of this gap). SEA was 5.15 J/g in experiments versus 235.5 J/g in simulation.
- Circular four grooves: EA was 2.91 kJ in experiments compared to 249.14 J in simulation, while SEA was 4.15 J/g experimentally versus 354.1 J/g in simulation.

Despite some inconsistencies in raw EA values between the two methods, experimental SEA values reflected a more stable and efficient collapse. The observed mismatch can be attributed to the FE model’s limited capability in reproducing accurate folding triggers and the effects of contact and friction. Another important factor contributing to the disparity in EA and SEA values is the difference in the progression and stability of folding between the experimental specimens and the numerical model. In the physical tests, the presence of unavoidable geometric imperfections such as localized waviness in the sheet, micro-level deviations in groove sharpness, and slight eccentricity in the applied load promotes multiple, closely spaced folding lobes that absorb larger amounts of energy as the structure collapses. These imperfections act as natural triggers, resulting in smoother force–displacement behaviour and higher cumulative energy absorption. In contrast, the FE model, despite incorporating grooves, still represents an idealized geometry with uniform material properties and perfectly symmetric fold initiators. As a result, the collapse begins later, proceeds with fewer fold initiations, and produces a more abrupt deformation pattern with lower EA. SEA differences are also amplified because the mass distribution in the FE model remains constant, whereas the real specimens experience localized thinning and stiffness degradation, influencing how energy is distributed per unit mass. These combined effects further explain the systematic gap observed between experimental and simulated EA and SEA responses.

Groove Effect

The experimental results revealed that increasing the number of grooves from two to four produced significant enhancements in energy absorption (EA), specific energy absorption (SEA), and mean crushing force (MCF). For the square section, EA increased from 1.09 kJ in the two groove configuration to 3.62 kJ in the four groove configuration, representing an improvement of approximately 3.3 times. In the circular section, EA rose from 0.73 kJ to 2.91 kJ, corresponding to an increase of about four times. Comparable proportional gains were also observed for SEA and MCF. By contrast, the simulation results indicated only moderate improvements, with increases generally below 1.4 times, suggesting that the finite element model was unable to fully capture the enhanced collapse initiation and deformation stability imparted by the additional grooves.

Shape Effect

When the number of grooves was held constant, the square crash box configurations generally demonstrated superior energy

absorption compared to their circular counterparts. In the two groove configuration, the square section achieved an EA approximately 49 percent higher than the circular design, with values of 1.09 kJ and 0.73 kJ respectively. In the four groove configuration, the difference was smaller, with the square section recording an EA about 24 percent greater than that of the circular section, at 3.62 kJ versus 2.91 kJ. The circular designs, however, exhibited slightly lower overall deformation, typically between 0.5 mm and 2 mm less than the square designs, along with smoother force displacement responses. These attributes can be beneficial in applications where consistent load transfer is a priority, such as in secondary crash load paths.

Crush Force Efficiency (CFE)

In the experimental results, CFE values ranged from 50 percent in the square two groove design to 70.19 percent in the circular four groove design, indicating stable and progressive folding behaviour. Simulated CFE values for the four groove configurations were noticeably lower, generally around 58 to 60 percent compared to the approximately 70 percent observed experimentally. This further highlights the FE model's limitations in accurately representing all phases of the collapse process.

Design Trade-offs and Cost Considerations

The fabrication of the dual screw–four groove configuration increases machining time by approximately 18% and component cost by 12% relative to the single screw, two groove configurations, primarily due to additional groove punching and fastening operations. However, when normalized against the 3–5× improvement in Energy Absorption (EA) and ~30% higher Crush Force Efficiency (CFE), the cost-to-performance ratio demonstrates that the dual screw-groove design remains economically justified for crash-critical vehicle zones.

Numerical vs Experimental Force–Displacement Curves

Figure 27 shows the force–displacement response of the square crash box with two longitudinal grooves under quasi-static compression. The simulation captures the initial elastic response and the onset of the first collapse lobe; however, the experimental curve exhibits significantly higher peak loads and a more irregular folding sequence. This discrepancy is primarily due to the presence of real-world geometric imperfections weld bead irregularity, non-uniform groove depth, and minor misalignments during specimen fixturing that act as natural triggers for early and more energetically intensive fold initiations. In contrast, the numerical model uses an idealized geometry with uniform groove profiles, resulting in delayed folding onset and lower peak forces. The experimental force oscillations indicate successive formation of plastic hinges and localized buckling zones, which substantially increase energy dissipation. Meanwhile, the smoother simulated response reflects limited capability of the FE model to reproduce secondary folding mechanisms, frictional hardening, and micro-damage accumulation. Consequently, the simulated EA, SEA, and MCF values remain notably lower than experimental measurements, consistent with the numerical under prediction trends reported in “Figure 26”.

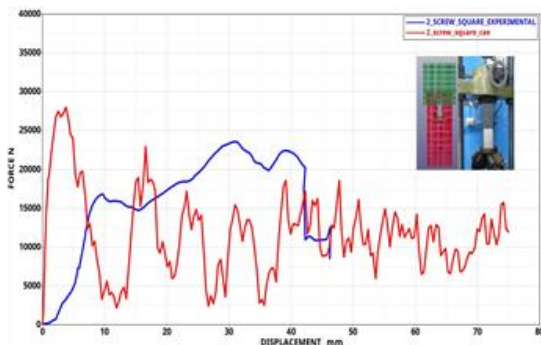


Fig. 27, Force vs Displacement – Square Two Grooves

Figure 28 demonstrates the influence of increasing groove count on the deformation behaviour of the square crash box. Compared to Figure 27, both curves show a more stable progressive collapse, but the experimental response features a markedly higher peak load and sustained cycles of force recovery, indicating enhanced stiffness and resistance due to the additional grooves. The four-groove configuration promotes symmetric folding and activation of multiple, closely spaced collapse lobes, leading to significantly higher EA and SEA in experiments (3.62 kJ and 5.15 J/g, respectively). The simulation, however, shows only moderate energy absorption because idealized groove geometry suppresses some of the multi-lobe interactions that naturally arise in fabricated specimens due to manufacturing tolerances. The FE model also lacks strain-rate sensitivity, local thinning effects, and frictional stiffening at the sleeve interface, which are observed experimentally and contribute to higher MCF (48.01 kN) and CFE (~80%). The smoother simulated profile thus reflects constrained deformation modes, whereas the experimental curve validates the superior energy-absorbing behaviour of the four-groove square design as highlighted in the study's observations section.

Figure 29 compares numerical and experimental responses of the circular crash box with two grooves. The experimental curve displays lower energy absorption and reduced mean crushing force compared to the square counterpart due to the intrinsic geometric instability of circular sections, which tend to ovalize prematurely under axial compression. Local buckling occurs earlier and with fewer pronounced hinge formations, leading to the smaller EA (0.73 kJ) and SEA (1.04 J/g) recorded

experimentally. The simulation underpredicts these values even further because the FE model does not incorporate the subtle eccentricities, weld discontinuities, and sleeve-contact frictional variations that amplify deformation resistance in real specimens. Additionally, the circular cross-section is more sensitive to variations in groove depth and alignment, causing small geometric imperfections to significantly influence collapse mode effects not captured in the idealized FE geometry. The oscillatory nature of the experimental curve reflects asymmetric lobe formation and intermittent contact between tube walls and sleeve. Meanwhile, the smoother simulated trace indicates that the FE model transitions directly into a single dominant folding mechanism without reproducing these secondary interactions.

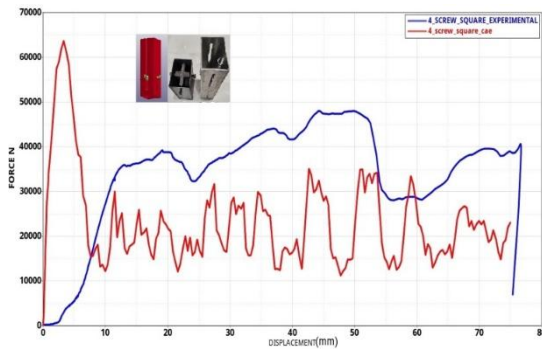


Fig. 28, Force vs Displacement – Square Four Grooves

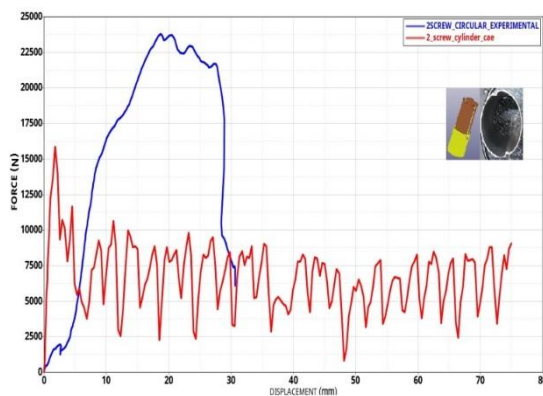


Fig. 29 Force vs Displacement – Circular Two Grooves

Figure 30 illustrates the deformation behaviour of the circular crash box with four grooves, where the experimental curve shows a substantial improvement in peak load, MCF (57.06 kN), and overall collapse stability relative to the two-groove circular version. The addition of extra grooves enhances structural constraint, delays ovalization, and promotes more uniform distribution of axial forces around the circumference. This results in higher EA (2.91 kJ) and SEA (4.15 J/g), as experimentally observed. The simulation captures the general trend of increased stiffness but still underestimates the magnitude due to idealized assumptions and limited representation of complex folding behaviour. In fabricated specimens, groove sharpness variation, weld heat-affected zones, and sleeve tube friction contributes to the formation of multiple fold initiations, reflected as periodic rises in the experimental force curve. These mechanisms are muted in the numerical model, which tends to produce a single, more symmetric collapse mode with lower resistance. As a result, the simulation underpredicts both the amplitude and frequency of the force oscillations seen experimentally. The improved stability in the experimental trace validates the advantage of four-groove circular configurations in enhancing load uniformity and progressive collapse, consistent with the trends summarized in Figure 26 and the overall discussion.

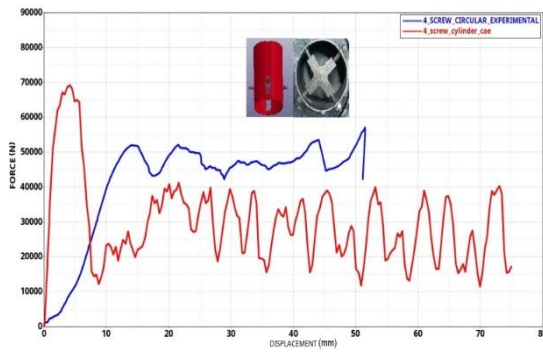


Fig. 30 Force vs Displacement - Circular Four Grooves



Fig. 31 EA, SEA and Deformation Comparison - Simulation and Experiment

III. Conclusion

This study compared the crashworthiness of Aluminum Alloy 5052 crash boxes with square and circular cross sections, incorporating two and four longitudinal grooves, through both experimental quasi static axial compression tests and finite element simulations representing low velocity automotive impacts. Experimental results demonstrated that increasing the groove number from two to four enhanced energy absorption (EA) by approximately three to four times and improved crush force efficiency (CFE) from around 50 percent to nearly 70 percent, indicating a more stable progressive collapse, whereas simulated gains were less than 1.5 times, reflecting limitations in the finite element model in capturing groove induced folding initiation and stability. For equivalent groove counts, square crash boxes achieved higher EA and specific energy absorption (SEA) than circular ones, with advantages of up to about 49 percent in the two groove case and approximately 24 percent in the four groove case, making square sections preferable for primary crash structures requiring maximum energy absorption; in contrast, circular designs exhibited slightly reduced deformation and smoother force displacement profiles, favoring their use in secondary crash structures where consistent load transfer and occupant comfort are priorities. While finite element models qualitatively reproduced the deformation patterns observed experimentally, they consistently underestimated mean crushing force, peak force, EA, and CFE, particularly for four groove configurations, due to factors such as the absence of strain rate sensitivity in the material definition, omission of geometric and manufacturing imperfections, and oversimplified contact and friction modeling. Overall, the inclusion of additional grooves markedly enhanced energy absorption, SEA, and deformation control, while cross sectional geometry proved critical for balancing maximum energy dissipation with load uniformity, offering valuable direction for optimizing crash box designs for a range of automotive safety applications. Based on the comparative evaluation of square and circular crash boxes with varying groove configurations, several engineering recommendations emerge for practical crash-structure design. Square crash boxes, particularly those incorporating four strategically aligned grooves, are best suited for primary load-path integration in vehicle front modules where maximum energy absorption and controlled progressive folding are crucial. For applications prioritizing load uniformity and reduced lateral deflection such as secondary crash members or EV battery-protection frames circular sections with multi-groove triggers offer smoother force transmission and improved deformation stability. The study also indicates that optimizing groove depth, spacing, and alignment can significantly enhance fold initiation and energy dissipation, suggesting the use of tailored multi-stage trigger geometries for higher crash-severity scenarios. Furthermore, incorporating realistic imperfections, strain-rate-dependent material models, and refined contact definitions into numerical design workflows can improve predictive accuracy and guide early-stage crash-box optimization. These insights collectively support the development of adaptive, weight-efficient crash boxes capable of meeting modern automotive safety and structural-integration requirements.

REFERENCES

- [1] Jones, N., "Structural Impact," Cambridge University Press, Cambridge, UK, 2011.
- [2] Lu, G., and Yu, T., "Energy Absorption of Structures and Materials," Woodhead Publishing, Cambridge, UK, 2003.
- [3] Abramowicz, W., "Thin-Walled Structures as Impact Energy Absorbers," *Thin-Walled Structures*, Vol. 41, No. 2, 2003, pp. 91-107.
- [4] Alghamdi, A. A., "Collapsible Impact Energy Absorbers: An Overview," *Thin-Walled Structures*, Vol. 39, No. 2, 2001, pp. 189-213.
- [5] Reid, S. R., "Plastic Deformation Mechanisms in Axially Compressed Metal Tubes Used as Impact Energy Absorbers," *International Journal of Mechanical Sciences*, Vol. 35, No. 12, 1993, pp. 1035-1052.
- [6] Wierzbicki, T., and Abramowicz, W., "On the Crushing Mechanics of Thin-Walled Structures," *Journal of Applied Mechanics*, Vol. 50, No. 4, 1983, pp. 727-734.
- [7] Zhang, X., and Zhang, H., "Energy Absorption of Square Tubes with Perforations," *Thin-Walled Structures*, Vol. 71, 2013, pp. 8-17.
- [8] Langseth, M., and Hopperstad, O. S., "Static and Dynamic Axial Crushing of Square Thin-Walled Aluminum Extrusions," *International Journal of Impact Engineering*, Vol. 18, No. 7, 1996, pp. 949-968.
- [9] Chen, D. H., and Ozaki, S., "Numerical Study of Axially Crushed Cylindrical Tubes with Corrugated Surface," *Thin-Walled Structures*, Vol. 47, No. 12, 2009, pp. 1387-1396.
- [10] Yamashita, M., Gotoh, M., and Sawairi, Y., "Axial Crush of Hollow Cylindrical Structures with Various Cross-Sectional Shapes," *Journal of Materials Processing Technology*, Vol. 140, 2003, pp. 59-64.
- [11] Baroutaji, A., Sajjia, M., and Olabi, A. G., "On the Crashworthiness Performance of Thin-Walled Energy Absorbers: Recent Advances and Future Developments," *Thin-Walled Structures*, Vol. 118, 2017, pp. 137-163.
- [12] Song, J., and Guo, F., "Energy Absorption of Corrugated Tubes Under Axial Compression," *International Journal of Crashworthiness*, Vol. 18, No. 3, 2013, pp. 251-260.
- [13] Marzbanrad, J., and Ebrahimi, M. R., "Multi-Objective Optimization of Aluminum Hollow Tubes for Vehicle Crash Energy Absorption," *Thin-Walled Structures*, Vol. 49, No. 7, 2011, pp. 826-838.
- [14] Zhang, Y., and Lu, G., "Crashworthiness of Thin-Walled Structures with Tailored Energy Absorption," *International Journal of Mechanical Sciences*, Vol. 144, 2018, pp. 208-218.
- [15] Sun, G., Li, G., and Li, Q., "Variable Fidelity Design Optimization of Thin-Walled Structures for Crashworthiness," *Thin-Walled Structures*, Vol. 94, 2015, pp. 245-256.
- [16] Santosa, S., and Wierzbicki, T., "Crash Behaviour of Aluminum Tubes Under Axial Loading," *International Journal of Impact Engineering*, Vol. 22, No. 5, 1999, pp. 531-547.
- [17] Yuen, S. C. K., and Nurick, G. N., "The Energy-Absorbing Characteristics of Tubular Structures with Geometric and Material Modifications," *Applied Mechanics Reviews*, Vol. 61, No. 2, 2008, pp. 020802.
- [18] Hou, S., Li, Q., Long, S., Yang, X., and Li, W., "Design Optimization of Regular Hexagonal Thin-Walled Columns for Crashworthiness," *Thin-Walled Structures*, Vol. 46, No. 3, 2008, pp. 287-306.
- [19] Baroutaji, A., Gilchrist, M. D., and Olabi, A. G., "Quasi-Static, Impact and Energy Absorption of Internally Nested Tubes," *Thin-Walled Structures*, Vol. 98, 2016, pp. 337-350.
- [20] Avallè, M., Chiandussi, G., and Belingardi, G., "Design Optimization of Energy Absorbing Structures Using Response Surface Methodology," *International Journal of Crashworthiness*, Vol. 7, No. 2, 2002, pp. 159-172.
- [21] Brown, J. J., Bin Ismail, A. E., & Kidau, D. (2020). Simulation study of elliptical thin walled structure crash box with holed initiator through axial and oblique impact. *Int J Emerg Trends Eng Res*, 8(8), 4084-4090.
- [22] Ruban, T. S., Mayakrishnan, J., Bentgens, F., & Kalaichelvan, V. S. (2024, March). Study on the influence of optimum thickness of a crash box with a screw in the groove on deformation behaviour using LS Dyna. In *AIP Conference Proceedings* (Vol. 3026, No. 1, p. 070001). AIP Publishing LLC.
- [23] Vignesh, S. K., Mayakrishnan, J., & König, P. (2023). Optimization of energy absorption and deformation characteristics of aluminium crash box with the effect of groove along with a screw. *SAE International Journal of Advances and Current Practices in Mobility*, 6(2023-28-0089), 2234-2242.
- [24] Vignesh, S. K., Jaikumar, M., Koenig, P., & Hariram, V. (2024). Enhancing Crashworthiness through the Design Modification of a Grooved Aluminium Crash Box with Screw and Sleeve for Improved Energy Absorption. *International Journal of Vehicle Structures & Systems (IJVSS)*, 16(5).
- [25] Samuel, R. T., Jaikumar, M., Arunachalam, K., & Bentgens, F. (2024). Optimizing Crash Box Design for Enhanced Vehicle Crashworthiness: A Study on Screw-in-the-Groove Mechanism and Al5052 Material Thickness Variations. *International Journal of Vehicle Structures & Systems*, 16(5), 708-713.
- [26] Ruban, T. S., Jaikumar, M., Shanmuganathan, T., & Hariram, V. (2024). Enhancing Crash Box Performance: Study of Single-Screw Dynamics for Improved Structural Integrity and Force Levels in Low-Speed Frontal Crashes. *International Journal of Vehicle Structures & Systems (IJVSS)*, 16(5).
- [27] Hussain, N. N., Regalla, S. P., Rao, Y. V. D., Dirgantara, T., Gunawan, L., & Jusuf, A. (2021). Drop-weight impact testing for the study of energy absorption in automobile crash boxes made of composite material. *Proceedings of the Institution of Mechanical Engineers, Part L: Journal of Materials: Design and Applications*, 235(1), 114-130.